

---

# Planetary Nebulae around [WC] stars: morphologies and kinematics

Miriam Peña

Instituto de Astronomía, Universidad Nacional Autónoma de México, Ciudad  
Universitaria, México D.F. 04510, México [miriam@astrocu.unam.mx](mailto:miriam@astrocu.unam.mx)

**Summary.** The morphology and kinematics of a large sample of planetary nebulae ionized by [WC] central stars is revised. It is found that the distribution of nebulae in the different morphological types (E, B, R, ...) is similar to the one for normal nebulae. However WRPNe seem to have more structures and inhomogeneities, as a consequence of the mechanical energy of the stellar wind. The analysis of the kinematics show that WRPNe are expanding faster (especially the more evolved objects) and present more turbulence, also as a consequence of the action of the stellar wind.

**Key words:** Planetary nebulae: general – ISM: kinematics and dynamics - Stars: winds, outflows

## 1 Introduction

About 10% of galactic planetary nebulae (PNe) are ionized by central stars presenting WR features of the C - sequence. We will call them WRPNe to distinguish them from the nebulae around not WR stars. A summary of the properties of the central stars can be found in Koesterke (2000). It is found that the mass loss rates go from  $10^{-6.7}$  to  $10^{-4.8} M_{\odot} \text{ yr}^{-1}$ , and the terminal velocities of the stellar winds are between several hundreds (in [WC-late] stars) to several thousands  $\text{km s}^{-1}$  (in [WC-early] stars). The effective temperature of the stars is closely related to their [WC] type, being between 30,000 and 60,000 K for the late ones ([WC] 11 - 6 and much hotter (from 80,000 to 100,000 K) for the early ones ([WC] 6 to [WO] 2). The spectral classification of the stars has been recently revised by Acker & Neiner (2003). Due to the large mass loss rates and terminal velocities, the mechanical energy of the [WC] winds are much larger than in the non-WR cases. This energy is deposited on the nebular shells affecting their shapes and kinematics. We will revise these properties for a large sample of WRPNe.

## 2 Nebular morphologies

The morphology of many WRPNe have been classified by, for instance, Gorny & Stasińska (1995) and other authors. Also some objects appear in the catalogue by Manchado et al.(1996). To perform a more complete classification and to analyze particular characteristics of nebulae, we revised all images of WRPNe obtained with the Hubble Space Telescope (HST). We found about 28 objects observed at high resolution with the HST. The list of objects with a revised morphological classification is presented in Table 1, where we also list several nebular and stellar characteristics for many WRPNe.

Regarding the morphologies, we can say that more than 60% of the WRPNe analyzed are elliptical, about 12-15% are bipolar, 5% are round, and the other categories (point-symmetric, quadrupolar, irregular) represent only a few % of the total sample. This is very similar to what it is found among non-WRPNe (Manchado et al. 1996). On the other hand, we found that all these objects present a very inhomogeneous structure (knots, rings, and filamentary structures) that not always can be characterized in the usual morphological descriptions. The more extended and spatially resolved objects show large-scale inner inhomogeneities (bubbles, rings, filaments, arcs, disks) and a number of them present external structures like extensions, ansae, FLIERS, BRETS, jets, ... (see Balick & Adam 2002 for a complete list and definition of these terms). Even the very compact and dense objects (with diameters smaller than a few arcsec), once resolved by HST or other ground telescopes, show structures and asymmetries similar to the ones presented by resolved evolved objects. In general it appears like non-WRPNe are smoother than WRPNe.

An excess of inhomogeneities and filamentary structures in WRPNe, in comparison with non-WRPNe, is expected as a consequence of the impact of the stellar wind. For instance, the hydrodynamical computations of García-Segura & McLow (1995) show that the expansion of a hot bubble pushed by a WR wind results in a filamentary broken shell with probably large turbulence. This effect is very difficult to quantify on the images, nevertheless we expect that the analysis of the velocity fields in both type of objects (WRPNe and non-WRPNe) sheds some light on this subject.

## 3 Nebular properties

Many studies of the nebular and stellar properties (including nebular abundances and kinematics, and analysis of the stellar wind) have been performed by different authors. The list is very extended. The interested reader can revise, e.g., Acker & Neiner (2003); Gesicki et al. (2006); Gorny et al. (2001); De Marco (2002); Koesterke (2001); Medina et al. (2006), and the references therein. Here we will address only a few aspects: How to derive the expansion velocities of nebulae and the relation of these velocities with stellar parameters as the stellar temperature and wind parameters. The data is mostly from the sample by Medina et al. (2006) plus additional data obtained recently by M. Peña, with the 6.5-m Magellan equipped with MIKE (the echelle spectrograph) in May 2006. This high-resolution spectrograph allowed us to obtain a large number of southern nebulae with very well resolved spectra. In total, our sample include 36 WRPNe and 23 non-WRPNe whose data are presented

**Table 1.** General characteristics of WRPNe

PNG	object <sup>a</sup>	morphol. <sup>a</sup>	$V_{\text{exp}}$	$\log N_e$	[WC]	$T_{\text{star}}$	$v_{\infty}$	$\log \dot{M}$	ref <sup>b</sup> .
001.5-06.7	SwSt 1*	G halo	12	4.48	9	35	400	-6.90	K01
002.2-09.4	Cn 1-5*	B: m	22.5	3.67	4	109	4867		AN03
002.4+05.8	NGC 6369*	E sm	35.5	3.5	4	150	1200	-6.15	K01
003.1+02.9	Hb 4*	P m	15.5	3.66	3-4	85	2059		AN03
004.9+04.9	M 1-25*	E m	22.5	4.01	6	56	1747		AN03
006.8+04.1	M 3-15*	P ms	17.5	3.87	5	55	1872		AN03
011.9+04.2	M 1-32	E	12.5	3.83	4-5		4867		AN03
012.2+04.9	PM 1-188*	R sm	30.5	2.9	10	35	360	-5.7	K01
017.9-04.8	M 3-30	E	26.9	2.72	2	49	2059		AN03
027.6+04.2	M 2-43*	E m	15	4	8	65	850	-6.08	K01
029.2-05.9	NGC 6751*	E sak	39.5	3.44	4	135	1600	-6.12	KH97
048.7+01.9	He 2-429	E a s	29	3.83	4		2371		AN03
060.4+01.5	HuDo 1		30	3.52	10	30			P05
061.4-09.5	NGC 6905*	E ask	41	3.18	2-3	141	1800	-6.32	K01
064.7+05.0	BD+30-3639*	E m	23.5	4.33	9	47	700	-4.87	K01
068.3-02.7	He 2-459*	E a?	30.5	4.24	8	77	1000	-5.01	K01
089.0+00.3	NGC 7026*	B: sm f	30.2	3.51	3	130	3500	-6.34	K01
096.3+02.3	K 3-61	E	30.5	3.22	4.5				
120.0+09.8	NGC 40*	E ask	25.5	3.3	8	78	1000	-5.62	K01
130.2+01.3	IC 1747*	E s	29	3.38	4	126	1800	-6.58	K01
144.5+06.5	NGC 1501*	Es	40.5	3.01	4	135	1800	-6.28	K01
146.7+07.6	M 4-18*	E sm	11.5	3.8	10	30.4	160	-6.05	K01
161.2-14.8	IC 2003	Es	21.4	3.58	3				
243.3-01.0	NGC 2452*	I sk	31.8	3.2	2	141	3000	-6.2	K01
278.1-05.9	NGC 2867*	E sm	27	3.42	2	141	1800	-6.24	K01
278.8+04.9	PB 6	R sk	38	3.43	2	140	3000	-6.25	K01
286.3+02.8	He 2-55	E	44	2.71	3	128	3000	-6.25	K01
291.3-26.2	Vo 1*	E: s	14	5	10	32	225		AN03
292.4+04.1	PB 8	E sk	14	3.65	5-6	33	1248		AN03
307.2-03.4	NGC 5189	I sk	27	2.69	2	135	3000	-6.30	K01
309.0-04.2	He 2-99	E s	37	2.76	9	49	900	-5.59	K01
309.1-04.3	NGC 5315*	Q	20	3.9	4	65			AN03
321.0+03.9	He 2-113*	B sm	20	4.24	10				
327.1-02.2	He 2-142*	E sm	16	4.5	9	35	884		AN03
332.9-09.9	CPD-56 8032*	E: s	14	4.7	10	34.5	225	-5.4	K01
337.4+01.6	Pe 1-7	E:	14	4.74	9	40	1872		AN03
352.9+11.4	K 2-16	E m	24	2.7	11	30	300	-6.36	K01
355.2-02.5	H 1-29	E:	24	3.67	4	77	2183		AN03
355.9-04.2	M 1-30*	B s	21	3.73	7				
358.3-21.3	IC 1297	E s		3.45	3	91	2933		

(a) Objects with \*: HST image, E:elliptical, B: bipolar, R: round, Q: quadrupolar, I: irregular. Small s: structure, m: multiple shells, a: ansae, k: knots.

(b) Stellar parameters are mostly from the compilation by Koesterke 2001 (K01). Other references are: AN03: Acker & Neiner 2003; KH97: Koesterke & Hamann (1997); P05: Peña 2005.

in Table 1. Effective temperature of the [WC] stars are taken from Non-LTE expansion atmosphere models from the literature, when available. Other references (given in Table 1) have been also used.

### 3.1 Density vs. Stellar temperature

As already known, nebular density diminishes with increasing stellar temperature, indicating that nebulae around low  $T_{\text{star}}$  are younger. (see Acker et al. 1996 and Fig.1 of Peña et al. 2001; also). It has been established that the above statement is true for almost all the WRPNe. Nebulae around hot stars (early [WC]s) have lower density than nebulae around colder stars (late [WC]s) except for a few nebulae around cold stars which show very low density. These ones have been identified as possible born-again AGB (Acker et al. 1996). Alternatively Gorny & Tylenda (2000) and Peña et al. (2001) suggest that they could be slowly evolving objects. In our sample these objects are PM1-188, K2-16 and He2-99, and it results interesting revised their morphology: all of them posses round or elliptical extended shells. PM1-188 in addition has an internal bipolar structure. They also have large expansion velocities for their spectral types (see Table 1).

### 3.2 Expansion velocities, $V_{\text{exp}}$

$V_{\text{exp}}$  is measured using the nebular line profiles. Very high spectral resolution is required and the slit position should be well defined. Inside the nebula there are density, thermal and ionization structures, a velocity field, a velocity gradient, turbulence, etc., complicating the definition of  $V_{\text{exp}}$ . Then, each author proposes his own definition. We use the following:

- 1) Spectra should be obtained at the central star position (center of the nebula).
- 2) [O III] 5007 or  $H\beta$  are used (after subtracting the thermal broadening) to measure  $V_{\text{exp}}$ .
- 3) For double-peak profiles,  $V_{\text{exp}}$  is half the difference from peak-to-peak and turbulence is estimated from the individual line widths.
- 4) For single profiles (which occurs for compact and small nebulae, with low  $V_{\text{exp}}$ ), half the line width is measured. In this case  $V_{\text{exp}}$  and turbulence are mixed.

Our values (in  $\text{km s}^{-1}$ ) are listed in column 4 of Table 1. We found that in general our values compare well (within 20%) with measurements by other authors.

## 4 Expansion velocities and stellar temperatures

Fig. 1 shows the measured  $V_{\text{exp}}$  as a function of the stellar temperature  $T_{\text{star}}$ . We are including WRPNe (from Table 1) and non-WRPNe (from Medina et al. 2006 data) and use different symbols for double-peak or single profile objects. The figure is an adaptation of a similar figure from Medina et al. (2006) and it shows that:

- 1) At any stellar temperatures, WRPNe show larger expansion velocities than non-WRPNe. Certainly, this should be a consequence of the mechanical energy of the stellar wind blowing on the shell.

- 2) For all type of PNe (WRPNe and non-WRPNe),  $V_{\text{exp}}$  increases with the stellar temperature. As  $T_{\text{star}}$  is indicative of the stellar age, this behavior shows that  $V_{\text{exp}}$

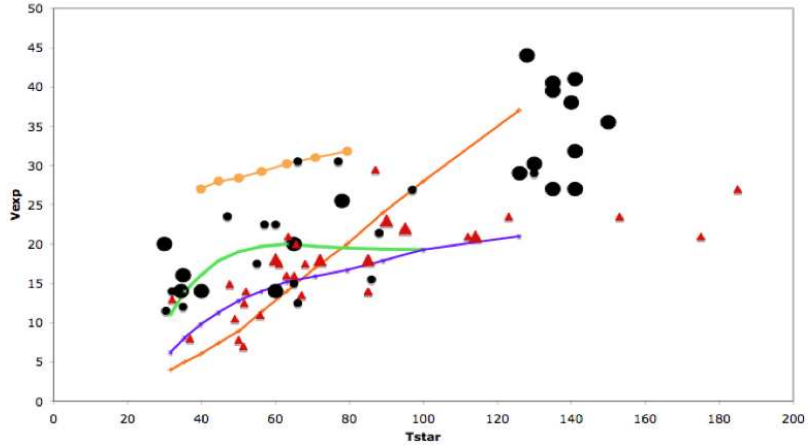


**Fig. 1.** Expansion velocity as a function of the stellar temperature. Large (small) symbols represent nebulae with double (single) peak profiles. Black dots are WRPNe, red rectangles are non-WRPNe. The lines represent the behavior of hydrodynamical models computed by Schoenberner et al. 2005, for a star of  $0.595 M_{\odot}$  and initial expansion velocity,  $V_{\text{AGB}} = 10 \text{ km s}^{-1}$ . Lines in green and blue present the model velocity for the rim and shell when the density is  $\rho \sim r^{-2}$ . Orange lines represent a model with  $\rho \sim r^{-3}$ .

increases with the age. This effect is much larger in WRPNe. For non-WRPNe,  $V_{\text{exp}}$  increases only to a maximum of about  $30 \text{ km s}^{-1}$ .

3) Born-again objects show very large  $V_{\text{exp}}$  considering their  $T_{\text{star}}$ . Of course this also occurs for slowly evolving objects. Thus their high  $V_{\text{exp}}$  is not indicative of the “born-again” phenomenon.

## 5 $V_{\text{exp}}$ and hydrodynamical models

In Fig. 1 we have included lines representing the evolution of  $V_{\text{exp}}$  as a function of  $T_{\text{star}}$  as given by an hydrodynamical model for a nebula with a star of  $0.595 M_{\odot}$ , initial expansion velocity at the AGB,  $V_{\text{AGB}} = 10 \text{ km/s}$  and two possible behaviors for the nebular density:  $\rho \sim r^{-2}$  and  $\rho \sim r^{-3}$ . The model is from Schoenberner et al. (2005). The graph indicates that:

1) Non-WRPNe and young WRPNe seem to follow the behavior of model with nebular density  $\rho \sim r^{-2}$ .

2) Evolved WRPNe are closer to the model with nebular density  $\rho \sim r^{-3}$  (steeper density structure), but probably a model with a larger  $V_{\text{AGB}}$  could also reproduce this behavior. We consider that this latter possibility is more adequate for WRPNe (Medina 2004).

## 6 Turbulence

From our data, turbulence can be estimated by measuring the FWHM of the blue and red components of double-peak profiles (single profile objects cannot be used for this). Our values are listed in Table 2. The data show that, WRPNe have larger FWHM than non-WRPNe. That is, in addition to higher  $V_{\text{exp}}$ , WRPNe also present more turbulence. Similarly large turbulence have been derived by, e.g., Gesicki et al. (1998; 2006), although from their models they do not find larger  $V_{\text{exp}}$  for their objects.

**Table 2.** Line widths for double peak objects

object	[WC]	$\Delta V1$	$\Delta V2$	object	[WC]*	$\Delta V1$	$\Delta V2$
NGC6369	4	24	28	He2-142	9	19	22
NGC6751	4	24	29	Pe1-7	9	33	30
NGC6905	2-3	25	27	K2-16	11	22	16
NGC7026	3	24	25	IC5217	–	16	20
NGC40	8	18	<15	NGC6567	–	< 20	< 20
NGC1501	4	20	19	NGC7009	–	< 15	< 15
NGC2867	2	24	23	NGC2022	–	16	20
PB6	2	18	20	PRMT1	–	24	23
He2-55	3	17	21	NGC4361	–	22	20
NGC5189	2	23	21				

\*. Objects without a [WC] type are non-WRPNe.

## 7 Conclusions

From the analysis of high-resolution imaging of WRPNe we found that nebulae around [WC] central stars are mostly asymmetrical and highly clumpy and filamentary. They present a lot of structure even when they are young and compact. The distribution of nebular morphologies are similar to the one for non-WRPNe: more than 60% are elliptical, 12-15% are bipolar, 5% are round. The other categories represent only a few % of the total sample.

When we analyze the velocity fields, it is found that WRPNe have larger expansion velocities and more turbulence than non-WRPNe. This is certainly a consequence of the larger mechanical energy of the [WC] wind which is deposited on the nebular shell.

We have compared the expansion velocities of the objects in our sample with the predictions of a hydrodynamical model by Schoenberner et al. (2005) we conclude that WRPNe should have had a steeper density structure ( $\rho \sim r^{-3}$ ) than non-WRPNe ( $\rho \sim r^{-2}$ ). Alternatively we propose that the initial expansion velocity,  $V_{\text{AGB}}$ , should have been larger for WRPNe.

## References

1. A. Acker, S. Gorny, & F. Cuisinier, *A&A*, **305**, 944 (1996)
2. B. Balick & F. Adam, *ARA&A*, **40**, 439 (2002)
3. O. De Marco, *IAU Symp* 209, p. 215 (2002)
4. G. García-Segura & M.-M. MacLow, *ApJ*, **455**, 160 (1995)
5. K. Gesicki, A. A. Zijlstra, A. Acker, et al. 2006. *A&A*, **451**, 925 (2006)
6. K. Gesicki, A. A. Zijlstra, A. Acker, & R. Szczerba, *A&A*, **329**, 265 (1998)
7. S. Gorny & G. Stasińska, *A&A*, **303**, 893 (1995)
8. S. Gorny & R. Tylenda, *A&A*, **362**, 1008 (2000)
9. S. Gorny . G. Stasińska, R. Szczerba, & Tylenda , *A&A*, **377**, 1007 (2001)
10. L. Koesterke *Ap&SS*, **275**, 41 (2001)
11. L. Koesterke & W.-R. Hamann, *A&A*, **320**, 91 (1997)
12. A. Manchado, M. Guerrero, L. Stanghellini, & M. Serra-Ricart: *The IAC Morphological Catalog of Northern Galactic Planetary Nebulae*, ed. by Instituto de Astrofísica de Canarias, 1996
13. S. Medina, Ph.D. Thesis, UNAM, México (2004)
14. S. Medina, M. Peña, G. Stasinska, *RevMexAA*, **42**, 53 (2006)
15. M. Peña, G. Stasińska, & S. Medina, *A&A*, **367**, 983 (2001)
16. M. Peña, *RevmexAA*, **41**, 425 (2005)
17. D. Schoenberner, R. Jacob, M. Steffen et al., *A&A*, **431**, 963 (2005)
18. R. Tylenda & G. Stasinska, *A&A*, **288**, 897 (1994)